

Synthesis and Characterization (Electrical and Optical) of TiO₂ doped with MnO₂

ABSTRACT

TiO₂ is vastly used in several industries due to its several properties, its wide bandgap and poor ionic conductivity has however hampered its application in the energy industry. In this work, TiO₂ has been doped with MnO₂ to produce thin films. The doping was carried out in 5, 10 and 15 wt% of MnO₂ and the resultant films characterized (uv/vis photospectroscopy and 4-point probe conductivity test). It was observed that the electrical conductivity was highly improved as was observed in the conductivity test which showed the conductivity of pure TiO₂ at 0.0100Ω⁻¹m⁻¹, increase to 0.0217 Ω⁻¹m⁻¹ at 5wt% of MnO₂, and to 0.0409Ω⁻¹m⁻¹ at 10wt% and finally to 0.0749wt Ω⁻¹m⁻¹ at 15wt% of MnO₂. The improvement in the conducting properties were also made evident by the drastic reduction in the bandgap energy of TiO₂ which reduced for 3.2eV of pure TiO₂ to 2.7eV, 2.2eV and 1.7eV for 5wt%, 10wt% and 15wt% MnO₂ respectively. These bandgap values were obtained from kebulka-monk plots made by the reflectance readings of the UV/VIS.

Keywords: [Doping, Conductivity, TiO₂, Bandgap]

1. INTRODUCTION

Titanium dioxide (TiO₂) is about the most popular white pigment, and this can be attributed to its high refractive index which has made it found vast applications in coatings, photocatalysis, solar cells among others (Rao et al., 2016). TiO₂ like carbon has attracted lots of interest in recent years as a potent anode material for Li-ion batteries. Its environmental benignity, availability, small volume change during charge-discharge cycles(<4%) and low cost has made it attractive for the production of high power lithium-ion batteries. (Liu and Yang,2016).

However, its structural instability and poor ionic conductivity has stood out as a major setback. To circumvent this challenge, different forms of composites, alloying and doping has been done including nanocrystallization, all aimed at improving its characteristics.

Dong et al., (2013), prepared honeycomb-like porous TiO₂/GNs (graphene nano-sheets) composites as Li-ion anodes which reports enhancement of both the electric conductivity and structural stability of TiO₂. Based on their electrochemical and physical properties, different components are being combined with TiO₂ in order to achieve a perfect combination for energy related applications. Doping TiO₂ with ionic dopants such as Fe³⁺, Ti³⁺, Sn⁴⁺, etc has also been carried out by several researchers and showed improvement on the properties of TiO₂ especially improving its electrical conductivity.

For instance, Ren, et al.,(2014) used the solvothermal process at a low temperature to dope TiO₂ with Ti³⁺ and reported an increased electrochemical performance. Liu, et al.(2009) did a similar work by doping Ti³⁺ with TiO₂ nanotube arrays and reported an improvement on the lithium-ion intercalation capabilities of the doped anode material.

Metal oxides have not been exempted in this attempt. Among various oxides used so far are MoO₃, V₂O₅, CoO, SnO₂, etc.(Armstrong, et al. 2013). These reports suggest that the

37 metallic oxide coatings, not only led to almost zero volume change during cycling but also
38 inhibit pulverization as well as improve li-ion insertion/de-insertion properties of TiO₂ when
39 used as an anode material in Li-ion battery applications. Asahi et al.,(2001) report a
40 narrowed bandgap for TiO₂ when doped with Nitrogen. Zhao et al.,(2008) on further
41 investigation of N-TiO₂ discovered shallow acceptor states which existed slightly above its
42 valence state, while Vanadium-doped TiO₂ showed a red-shift in its spectra when studied
43 under UV-VIS spectrophotometer with high photodegradation activity than its pure TiO₂
44 counterpart Wu et al.,(2004).

45
46 In this work, MnO₂ is doped with TiO₂ in an attempt to improve the structural stability and
47 electrical properties of TiO₂.

48 **2. EXPERIMENTAL DETAILS**

49

50 **2.1 Synthesis Of Sol Gel Titania**

51 About 7.38g of TiCl₄ was added to 100mL of H₂O at 9°C under vigorous stirring for
52 30minutes. At the end, the H₂O temperature rose to 21°C. It was then rinsed by
53 centrifugation at 400rpm for 10 minutes. Then, 16mls of Ammonia solution was added first to
54 the solution before 10mL was later added to make 26mL of ammonia solution.

55 After centrifuging for 5 minutes, the supernatant is discarded and the residue retained and
56 mixed with more water and then centrifuged again. This process was repeated 10 times
57 using a total of 250mL of distilled water.

58 The volume of the mixture was made up to 50mL by adding water. Furthermore, 20mL of
59 30wt% of HCl was added to the solution and stirred vigorously and at this point the solution
60 became colourless. It was allowed to undergo Ostwald's ripening (Liu and Hu, 2020) for
61 24hrs at room temperature. Finally, the sol was centrifuged at 4000rpm to remove oversized
62 particles.

63

64

65 **2.2 Synthesis Of MnO₂**

66

67 About 8g of KMnO₄ was added to 38ml of 35% HCl. The temperature of the mixture was
68 raised to 70°C and held for 3hrs.

69 In a separate 250ml beaker, 5g of Na₂CO₃ (All materials are analytical grade) was measured
70 and enough water added to make a saturated solution. At this point, the solutions (in beaker
71 1 and 2) are mixed together resulting in the formation of insoluble MnCO₃ (manganese
72 carbonate).



74 The manganese carbonate is purified by centrifugation at 4500rpm, the supernatant is
75 discarded and the residue is stirred with water. This is washed with methanol and
76 centrifuged. This is repeated twice at 4500rpm. This is dried in a drying dish. The dried
77 material is dissolved in nitric acid (50%). 2ml of the solution is extracted, calcined at 500°C
78 and weighed. 2ml of the Mn(NO₃) contains 0.27g of MnO₂, with further dilution with water
79 0.16g of MnO₂ was gotten.

80

81 **2.3 Preparation of TiO₂ and MnO₂ Thin Films**

82 Slot coating (or Dr Blading) method of deposition was used to prepare the thin films on a
83 glass substrate. 0.02g/mol of TiO₂ mixed with 0.02g/mol of PVA (polyvinyl alcohol) and
84 stirred in a magnetic stirrer for about 10mins to make the mixture homogenous. The PVA is
85 added as a surface agent to enable the film stick to the surface of the slide. This mixture was
86 then deposited on the slide using the slot coating method and blow-dried with a hot air
87 blower. And the slide was further dried at about 200°C. Furthermore, 0.2ml MnO₂ and 0.2ml
88 of PVA was mixed together and stirred with a stirrer and this was also deposited on another

89 slide and dried. At this stage two thin films were prepared (a pure TiO₂ and pure MnO₂ thin
 90 films)

91

92 2.3 Preparation of MnO₂ Doped TiO₂ Thin Films.

93 About 1.9ml of TiO₂ was put in a beaker placed on a hot plate stirrer, 2ml of PVA was added
 94 and finally 5wt% of MnO₂ was gradually added to the mixture and allowed to stir mildly for
 95 5mins. This mixture was then deposited using the slot coating method on the slide and dried
 96 at 200⁰C. The process was repeated in preparing thin films for 10wt% and 15wt% of MnO₂

97

98 3. RESULTS AND DISCUSSION

99 The four point probe method was utilized to know the resistivity of the thin films. Table 1.0
 100 shows the obtained results and the corresponding conductivities.

101 **Table 1. Result of four-point probe test.**

102

Wafer_ID	Composition	Wafer Thickness	Resistivity(Ωm)	Conductivity (Ω ⁻¹ m ⁻¹)
Slide 1	TiO ₂ only	50nm	99.8923	0.0100
Slide 2	TiO ₂ (5%wt MnO ₂)	"	45.9958	0.0217
Slide 3	TiO ₂ (10%wt MnO ₂)	"	24.4677	0.0409
Slide 4	TiO ₂ (15%wt MnO ₂)	"	13.3581	0.0749

103

104 From the table Slide 1 which was prepared with only TiO₂ showed high resistivity value of
 105 99.89 Ohm-meter which confirms the semiconductor status of the material. However based
 106 on the percentage of doping, significant reduction in the resistivity was observed at 5% ,
 107 10% and 15%.

108 Following the resistivity values, the formula;

$$109 \sigma = 1/\rho$$

1.1

110 Where, σ represents conductivity and ρ is the resistivity which is gotten from the
 111 resistivity test.

112

113 The corresponding conductivity values also as evaluated using equation 2.0 showed
 114 significant increments as its value increased from 0.01Ω⁻¹m⁻¹ in the pure phase to 0.07 in the
 115 15%wt doping.

116 On a close examination of table 1.0 we observe that the doping improved the conductivity of
 117 TiO₂. At 15%wt MnO₂ doping, the resistivity had dropped to 13.3581Ωm which produced a
 118 conductivity of 0.0749Ω⁻¹m⁻¹. Further increase of the doping percentage led to irregular
 119 readings which suggested that the doping can only go this far for effective use.

120 To further confirm the improved electrical properties, optical analysis was further carried out
 121 by utilizing the UV/VIS spectrophotometer. From the reflectance values acquired, the
 122 bandgap (eV) was estimated by adopting the kebulka-munk approach. By using equations
 123 1.2 and 1.3 below, the bandgap was estimated for each of the samples where eV values are
 124 the x-axis intercept of the plots.

$$125 \text{Band Gap Energy (E) = } hc/\lambda$$

1.2

126

127 h = Plank's constant = 6.626 x 10⁻³⁴ Joules sec

128 c= Speed of light= 3.0 x10⁸ meter/sec

129 λ = cut of wavelength which from the spectrophotometer = 300- 600nm

130 Band Gap Energy (E) = 1240/ λ (eV).

131 With 1eV = 1.6 x 10¹⁹ Joules

132 From the reflectance data acquired, the kebulka-munk (k/s) equation was used to plot
 133 corresponding graphs using Microsoft excel.

134

135
$$f(R) = \frac{(1-R^2)}{2R} = \frac{k}{s} \quad (\text{Piketech, 2011})$$

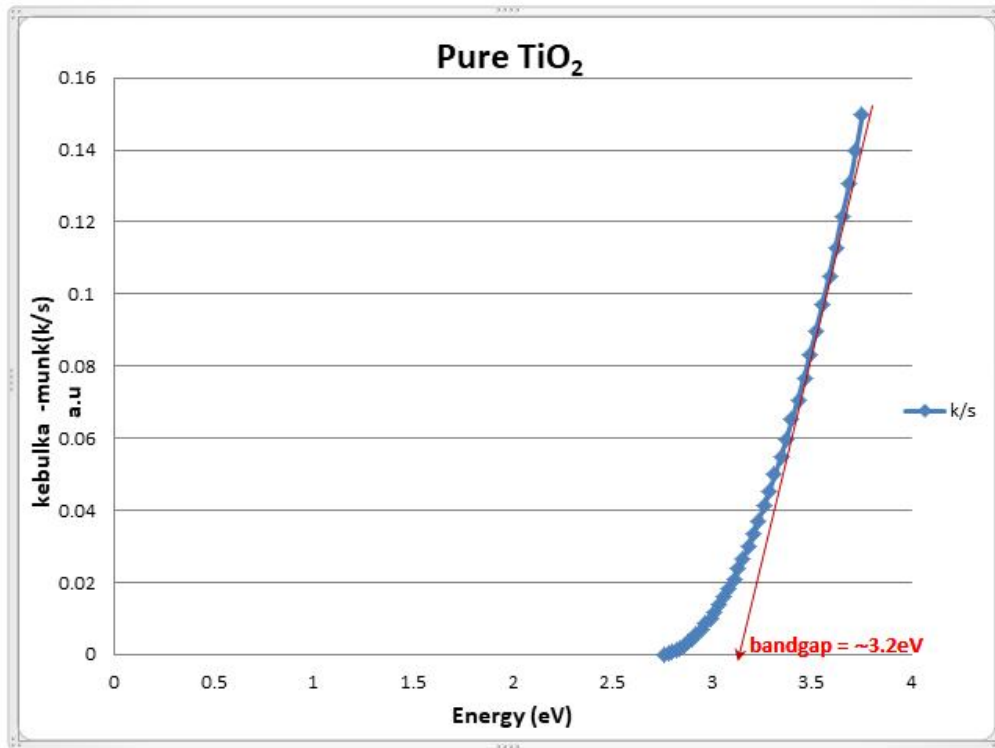
1.3

136 Where R represents the absolute Reflectance which is obtained from the percentage
137 reflectance value from the uv/vis data.

138 k is the absorption coefficient while s is scattering coefficient.

139 The general units of k/s is the absorption unit (a.u).

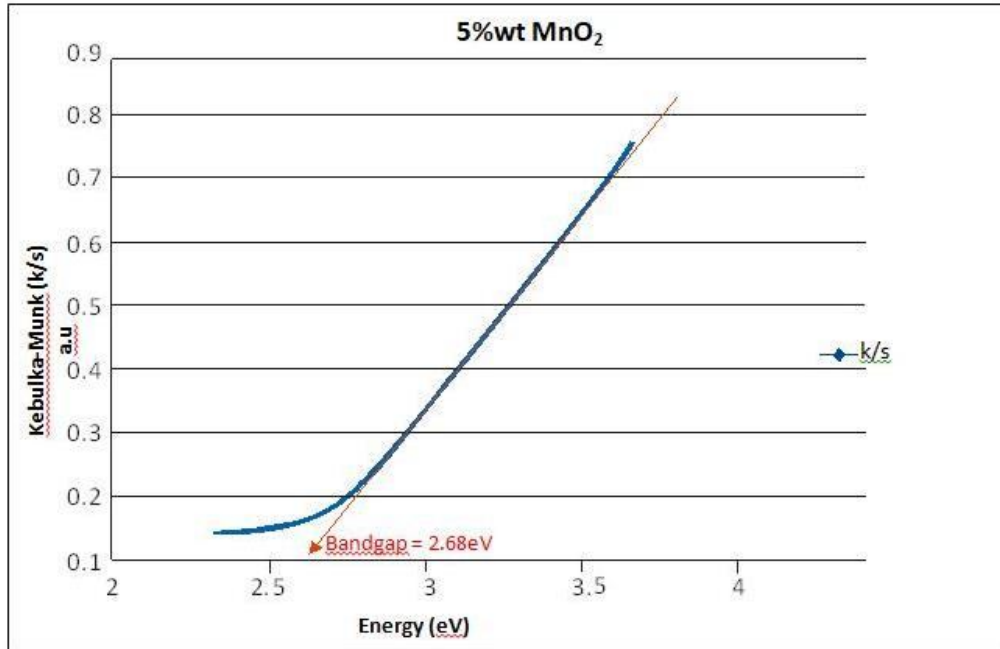
140



141

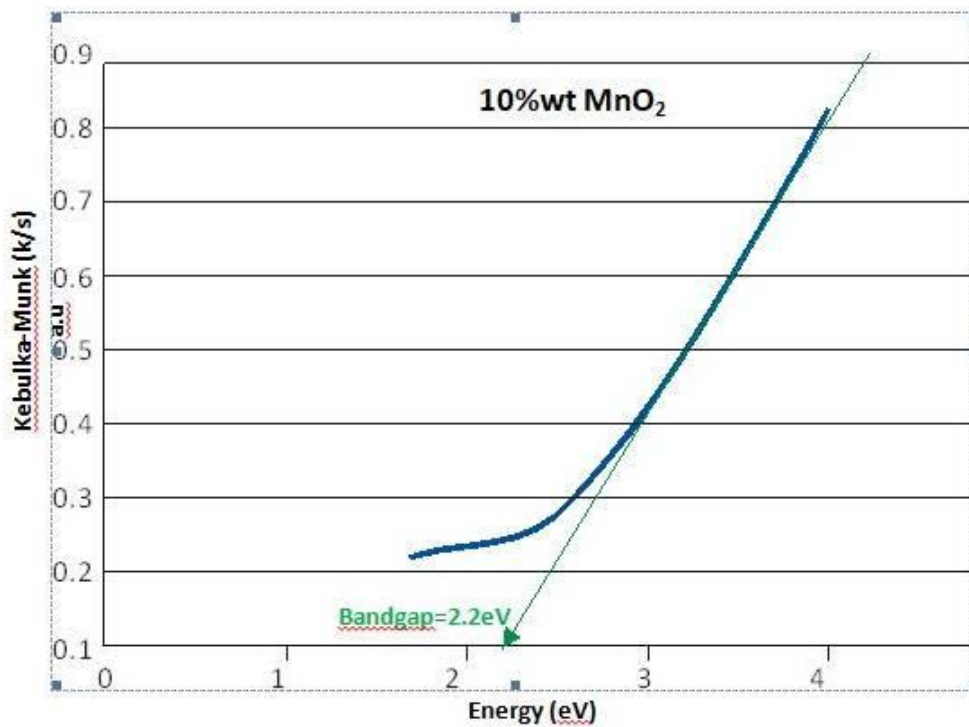
142

Fig. 1. Estimation of band gap value of pure TiO₂ using kebulka-munk plot



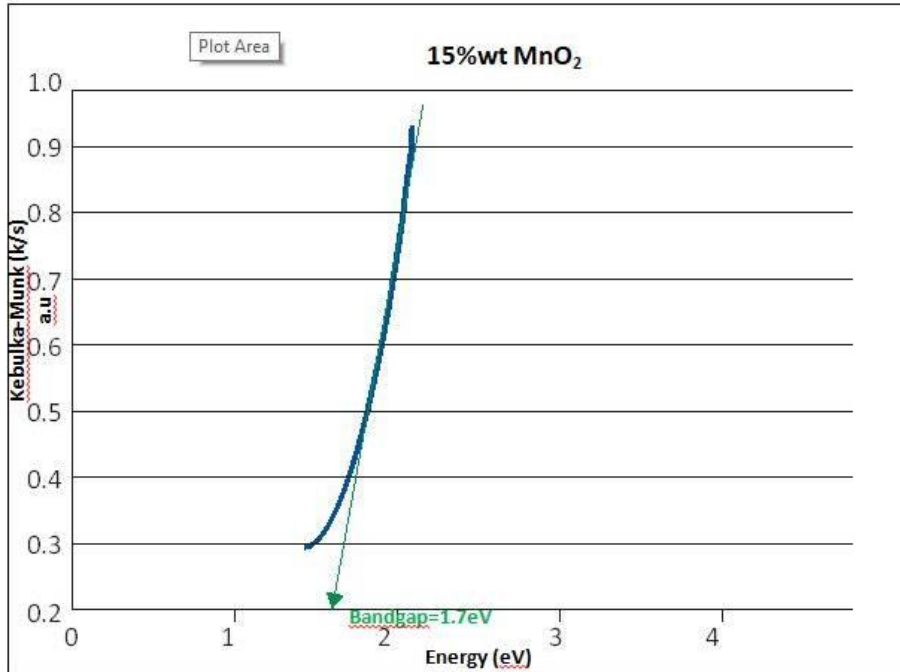
143
144
145
146

Fig.2. Estimation of band gap value of TiO₂ doped with 5%wt MnO₂ using kubelka-munk plot



147
148
149

Fig.3. Estimation of band gap value of TiO₂ doped with 10%wt MnO₂ using kubelka-munk plot



150
 151
 152
 153
 154
 155
 156
 157
 158
 159
 160
 161
 162
 163
 164
 165
 166
 167
 168
 169
 170
 171
 172
 173
 174
 175
 176
 177
 178

Fig. 4: Estimation of band gap value of TiO₂ doped with 15%wt MnO₂ using kebulka-munk plot

The UV/VIS analysis/characterization of the thin films gave clearer information on the impact of the MnO₂ doping on the TiO₂. Ordinarily, the latter comes with a very wide band gap of about 3.2eV (Dette et al., 2014) which makes it very difficult for electrons to travel from the valence band to the conduction band. It was observed that the band gap was appreciably reduced due to the effect of the doping as can be observed from fig 1 to fig 4. These are kebulka-munk plots which were done with the help of the % reflectance data gotten from the UV/VIS spectrophotometric reading using equations 1.2 and 1.3. Following the different doping percentages on the thin films, different band gap values were obtained (5%wt =2.7eV, 10%wt =2.2eV and 15%wt =1.7eV). These excellent optical results, corroborates an earlier work by Zhang et al.,(2009) which reported the impressive photocatalytic activity of MnO₂ doped TiO₂.

4. CONCLUSION

TiO₂ has shown very good characteristics which makes it a potent material for energy applications like li-ion batteries, and its credentials are improved obviously with decrease in particle size to the nano-scale, however its poor ionic conductivity had always hampered its use in the li-ion battery industry. This research has shown that if the right material is used for doping TiO₂, the electronic and ionic features can be greatly improved. MnO₂ was used because of its availability and ease of use in the doping process coupled with other known benefits of transition metal-oxides. The doping was done in 5%wt, 10%wt and 15%wt and was seen to improve both electrical and optical properties of the thin films.

179 **COMPETING INTERESTS**

180

181 Declaration of competing interest should be placed here. All authors must disclose any
182 financial and personal relationships with other people or organizations that could
183 inappropriately influence (bias) their work. Examples of potential conflicts of interest include
184 employment, consultancies, honoraria, paid expert testimony, patent
185 applications/registrations, and grants or other funding. If no such declaration has been made
186 by the authors, SDI reserves to assume and write this sentence: "Authors have declared that
187 no competing interests exist."

188

189 **AUTHORS' CONTRIBUTIONS**

190

191 Authors may use the following wordings for this section: " 'Author A' designed the study,
192 performed the statistical analysis, wrote the protocol, and wrote the first draft of the
193 manuscript. 'Author B' and 'Author C' managed the analyses of the study. 'Author C'
194 managed the literature searches..... All authors read and approved the final manuscript."

195

196 **REFERENCES**

197 Armstrong, M.J., Burke, D.M., Gabriel, T.(2013). "*Carbon nanocage supported synthesis of*
198 *V₂O₅ nanorods and V₂O₅/TiO₂ nanocomposites for Li-ion batteries.*" Journal of
199 Materials Chemistry 1(40):12568–12578.

200

201 Asahi R, Morikawa T, Ohwaki T, Aoki K, Taga Y.(2001) Visible-light photocatalysis in
202 nitrogen-doped titanium dioxide. Science 2001; 293: 269-271

203

204 Dette, C. Perez-Osorio, M.A., Kley, C.S., Punke, P., Patrick, C.E., Jacobson, P., Guistino, F.,
205 Jung, S.J., Kern, K. (2014). *TiO₂ anatase with a bandgap in the visible region.*
206 [Nano Letters](#), 14(11):6533-8, doi: 10.1021/nl503131s

207

208 Dong, D., Qin,L., Zheng ,M. (2013). *Preparation and electrochemical performances of*
209 *TiO₂/GNS composites as anode material for high-power lithium-ion batteries.*
210 1120, 224th ECS meeting(2013).

211

212 Liu, Y and Yang, Y (2016) *Recent Progress of TiO₂-Based Anodes for Li-ion Batteries.*
213 Journal of Nanomaterials Volume 2016 (2016), Article ID 8123652, 15 pages
214 <http://dx.doi.org/10.1155/2016/8123652>

215

216 Liu B, Hiu X.(2020). Hollow Micro- and Nanomaterials: Synthesis and Applications. Micro
217 and Nano Technologies 2020, Pages 1-38

218

219 Liu, D., Zhang, Y., and Xiao, P(2009). "*TiO₂ nanotube arrays annealed in CO exhibiting high*
220 *performance for lithium ion intercalation*" Electrochimica Acta, vol. 54, no. 27,
221 pp. 6816–6820.

222

223 Piketech. 2011 <http://www.piketech.com/files/pdfs/DiffuseAN611.pdf>, extracted on the 14th of
224 January, 2016

225

226 Ren, Y., Li, J., and Yu, J.(2014). "*Enhanced electrochemical performance of TiO₂ by Ti³⁺*
227 *doping using a facile solvothermal method as anode materials for lithium-ion*
228 *batteries*" Electrochimica Acta, vol. 138, pp. 41–47.

229
230 Wu JC-S, Chen CH. A visible-light response vanadium-doped titania nanocatalyst by sol-gel
231 method. J Photochem Photobiol A 2004; 163: 509-515
232
233
234 Zhang, L., He, D., Jiang, P. (2009) MnO₂-doped anatase TiO₂ – An excellent
235 photocatalyst for degradation of organic contaminants in aqueous solution J.
236 Catalysis Communications 10(10), 1414 – 1416
237 Zhao Z, Liu Q. Mechanism of higher photocatalytic activity of anatase TiO₂ doped with
238 nitrogen under visible-light irradiation from density functional theory calculation.
239 J Phys D Appl Phys 2008; 41: 1-10.
240
241
242